Dalton Transactions

Accepted Manuscript

ROYAL SOCIETY OF CHEMISTRY

www.rsc.org/dalton

Dalton Transactions

Dynamic Article Links ►

Cite this: DOI: 10.1039/c0xx00000x

www.rsc.org/xxxxxx

ARTICLE TYPE

Two New Zinc(II) Coordination Complexes with Helix Characteristics Showing Both Interpenetration and Self-catenation Features: a Platform for Synthesis of Chiral and Catenated Structures Assembled by Length-Modulated Dicarboxylates

Yue Wang,[a]* Yan Qi[a], Vladislav A. Blatov[b,c], Jimin, Zheng[d], Qun Li[a] and Chao Zhang[a]

Received (in XXX, XXX) Xth XXXXXXXXX 20XX, Accepted Xth XXXXXXXXX 20XX
DOI: 10.1039/b000000x

Two new zinc coordination complexes, namely, $[Zn_2(tib)_{4/3}(L^1)_2]\cdot DMA$ (**1**) and $[Zn_2(tib)_{4/3}(L^2)_2]\cdot H_2O$ (**2**) (tib = 1,3,5-tris(1-imidazolyl)benzene, H_2L^1 = biphenyl-4,4'-dicarboxylic acid, H_2L^2 = 4,4'-(2,2'-oxybis(ethane-2,1-diyl)bis(oxy))dibenzoic acid and DMA = N,N-dimethylacetamide) are obtained by using achiral mixed-ligands and characterized by elemental analysis, IR and X-ray crystallography. Compounds **1** and **2** both display intriguing structural features of both interpenetration and self-catenation. By careful inspection of two structures, we found that Zn(II) cations, the tib ligands, and dicarboxylic anions show the same coordination modes or analogous configurations. Compound **1** is chiral, confirmed by measuring the optical rotation of bulk samples using solid-state circular dichroism (CD). It is comprised of two crystallographically independent interpenetrated 3D motifs, each containing interlaced triple-stranded right- and left-handed Zn–L^1–Zn helical chains, respectively, and chiral 2D $[Zn(tib)_{2/3}]$ layers. Both motifs display binodal (3,4)-coordinated 3D self-catenated networks with the point symbol $(10^3)_2(10^6)_3$ and vertex symbols $[10_{13}\cdot10_{13}\cdot10_{13}]$ and $[10_7\cdot10_7\cdot10_8\cdot10_{10}\cdot10_{11}\cdot10_{11}]$. However, two types of helical chains are not racemic due to the differences between two kinds of L^1 anions, and two types of chiral 2D $[Zn(tib)_{2/3}]^{2+}$ layers are not enantiomeric either due to the different configurations of tib ligands. Therefore, two motifs are not enantiomers. Compound **2** is achiral, containing the Zn–L^2–Zn zigzag chains that span into three directions and chiral 2D $[Zn(tib)_{2/3}]$ layers. The overall 3D network is a new binodal (3,4)-coordinated self-catenated network with the point symbol $(10^3)_2(10^6)_3$ and vertex symbols $[10_7\cdot10_7\cdot10_7]$ and $[10_2\cdot10_4\cdot10_5\cdot10_5\cdot10_5\cdot10_5]$. Two of these nets interpenetrate. Their chiral and achiral structures are mainly modulated by the length of dicarboxylates. As expected, compounds **1**-**2** have photoluminescence behaviors and compound **1** has ferroelectric behavior. The thermogravimetric studies of **1**-**2** have also been investigated. We examined all 48 known structures containing tib ligand and made a conclusion that the metal+tib combination modulated by prolonged L ligands can be a good platform for new chiral and catenated structures.

1. Introduction

Recently, the rational design and synthesis of chiral coordination complexes are active fields of crystal engineering not only because of their intriguing variety of architectures and topologies, but also by virtue of their potential applications in enantioselective catalysis and separation, nonlinear optics, ferroelectrics, and chiral magnets.[1,2] Consequently, many chiral coordination polymers have been generated by self-assembly processes.[3] These chiral MOFs have usually focused on two general synthetic strategies based on the ligands used: one is using chiral organic ligand as linker to connect metal centers, the other is using achiral ligand *via* spontaneous resolution. However, the products obtained by spontaneous resolution from achiral starting materials are normally a racemic mixture of chiral crystals, although each crystal is a single enantiomer.[4] Moreover, the flexibility of achiral molecular tectons is responsible for satisfying the needs for the formation of ultimate chiral frameworks, while the achiral rigid ligands *via* assembly with metal salts to crystallize in chiral space group with chiral structure are not well documented to date.[5]

Entangled systems are common in nature and a major theme of supramolecular chemistry.[6] Interpenetration is one of the most investigated type of entanglement;[7] interpenetrating motif includes several nets and cannot be separated without breaking of bonds. In contrast, self-catenated structures are based on single nets having the peculiarity that some rings of bonds are catenated by other rings belonging to the same net. To date, although considerable efforts have been directed to the construction of self-catenated nets, only a limited number of cases are known.[8-10] After all, the achievement of self-catenation continues to be a great challenge since it is comparatively difficult to predict the

target compound prior to synthesis.[9d] As was pointed out,[11] the multidimensional MOFs with large voids and low coordination number of metal centers tend to form interpenetration. In addition, long ligands, usually benefiting to form large voids, may be a good candidate to the formation of interpenetrated structures.[12] In particular, our previous studies using the transitional metal ions and achiral mix-ligands resulted in the entangled frameworks showing structure characteristics of chiral, helix, self-catenation as well as interpenetration, such as $[Co(L^3)_2(bimb)]$ (HL^3= 3,5-dinitrobenzoic acid, bimb= 1,4-bis(imidazol-1-yl)-butane)[13], a chiral polymer assembled from achiral components due to the presence of left-handed helices and $[Ni_3(L^4)_3(BTC)_2\cdot 2H_2O]\cdot 6H_2O$ (BTC=1,3,5-benzenetricarboxylate and L^4=1,4-bis(1-imidazolyl)benzene), a 3D self-catenated network[10b].

In order to obtain novel entangled systems, our synthesis strategy is to select mixed ligands similar to those in $[Ni_3(L^4)_3(BTC)_2\cdot 2H_2O]\cdot 6H_2O$. Thus we used 1,3,5-tris(1-imidazolyl)benzene (tib), a typical tripodal rigid ligand that have been used in the construction of MOFs with specific topologies and interesting properties,[14] biphenyl-4,4'-dicarboxylic acid (H_2L^1) and 4,4'-(2,2'-oxybis(ethane-2,1-diyl)bis(oxy))dibenzoic acid (H_2L^2) analogues of 1,4-benzenedicarboxylic acid that may induce ultimate structure with helicity and/or entanglement.[12,15] As the complexing atom we chose the Zn(II) ion that can usually have low coordination number of four with tetrahedral coordination geometry. As a result, two new compounds $[Zn_2(tib)_{4/3}(L^1)_2]\cdot$DMA (**1**) and $[Zn_2(tib)_{4/3}(L^2)_2]\cdot H_2O$ (**2**) (DMA = N,N-dimethylacetamide) were isolated successfully. Both compounds are characterized by elemental analysis, IR and X-ray crystallography. We have performed a detailed analysis of the crystal structures as well as topological analysis of all known structures of compounds containing tib ligand. The thermogravimetric studies of **1-2** have also been investigated. In addition, the ferroelectric property for **1** and their photoluminescence properties are discussed in detail.

2. Experimental

2.1. Materials and General Procedures

Solvents and starting materials for synthesis were purchased commercially and used as received. Elemental analysis for C, H and N was performed on a Perkin-Elmer 240 analyzer. The IR spectrum was recorded as KBr pellets on a Nicolet Magna-FT-IR 560 spectrometer in the 4000–400 cm^{-1} region. The thermogravimetric analyses were investigated on a standard TG analyzer under a nitrogen flow at a heating rate of 5 °C/min for all measurements. The photoluminescence measurements were carried out on crystalline samples at room temperature, and the spectra were collected with a Hitachi F-2500FL spectrophotometer. The solid-state circular dichroism (CD) spectra were recorded on a JASCO J-720S spectropolarimeter with KBr pellets. Electric hysteresis loops have been measured at ambient temperature by using a Premier II ferroelectric instrument.

2.2. X-ray Crystallographic Measurements for 1-2

Suitable single crystals of **1-2** were selected and mounted in air onto thin glass fibers. Accurate unit cell parameters were determined by a least-squares fit of 2θ values, and intensity data were measured on a Rigaku r-axis rapid IP area detector with Mo $K\alpha$ radiation (λ = 0.71073 Å) at room temperature. The intensities were corrected for Lorentz and polarization effects as well as for empirical absorption based on multiscan techniques; all structures were solved by direct methods and refined by full-matrix least-squares fitting on F^2 by SHELX-97. All nonhydrogen atoms were refined with anisotropic thermal parameters. Crystallographic data for compounds **1-2** are summarized in Table 1 and selected bond lengths and bond angles for compounds **1-2** are listed in Table S1 in ESI.

2.3. Synthesis of $[Zn_2(tib)_{4/3}(L^1)_2]\cdot$DMA (1)

A mixture of $Zn(NO_3)_2\bullet 6H_2O$ (0.30 g, 1.0 mmol), H_2L^1 (0.24 g, 1.0 mmol) and tib (0.28 g, 1.0 mmol) was dissolved in 8mL mixed water/DMA medium with volume ratio of 1:2 (water : DMA). The resulting mixture was then transferred and sealed in a 25 mL Teflon-lined stainless steel vessel, and heated at 170 ℃ for two days. After the reactor was slowly cooled to the room temperature, colorless block-shaped crystals were obtained. Yield: 45% (based on Zn). Elemental analysis (%): calcd for **1**: C 58.55, H 3.87, N 11.82. Found: C 58.58, H 3.92, N 11.78. Selected IR (KBr pellet, cm^{-1}): 1617 (s), 1507 (m), 1372 (s), 1242 (w), 1085 (m), 1072 (s), 1016 (m), 840 (m), 768 (s), 685 (m), 648(m).

2.4. Synthesis of $[Zn_2(tib)_{4/3}(L^2)_2]\cdot H_2O$ (2)

A mixture of $Zn(NO_3)_2\bullet 6H_2O$ (0.30 g, 1.0 mmol), H_2L^2 (0.35 g, 1.0 mmol) and tib (0.28 g, 1.0 mmol) was dissolved in 8mL mixed water/DMA medium with volume ratio of 1:2 (water : DMA). The resulting mixture was then transferred and sealed in a 25 mL Teflon-lined stainless steel vessel, and heated at 170 ℃ for two days. After the reactor was slowly cooled to the room temperature, colorless block-shaped crystals were obtained. Yield: 51% (based on Zn). Elemental analysis (%): calcd for **2**: C 58.98, H 4.42, N 9.82. Found: C 58.92, H 4.50, N 9.79. Selected IR (KBr pellet, cm^{-1}): 3423 (s), 3119 (m), 1610 (s), 1560 (s), 1508 (s), 1365 (s), 1241 (s), 1169 (m), 1132 (s), 1014 (m), 917(m), 817 (m), 780(s), 691 (m), 648 (s).

Table 1 Crystal Data and Structure Refinements for Complexes **1-2**

compound	**1**	**2**
formula	$C_{52}H_{41}N_9O_9Zn_2$	$C_{56}H_{48}N_8O_{15}Zn_2$
Fw	1066.72	1203.8
T (K)	293(2)	293(2)
crystal system	trigonal	trigonal
space group	*P3*	*R-3c*
a (Å)	19.106(3)	18.772(3)
b (Å)	19.106(3)	18.772(3)
c (Å)	11.496(2)	84.147(17)
V (Å^3)	3634.3(10)	25680(8)
Z	3	18
calcd *D* (g/cm^3)	1.462	1.401
F(000)	1644	10150
reflns	34777 / 11073	66249 / 6545
collected/unique	R(int) = 0.1525	R(int) = 0.1836
GOF	0.967	1.024
final *R* [$I > 2\sigma(I)$]	R1 = 0.0730, wR2 = 0.1380	R1 = 0.0902, wR2 = 0.1992

3. Results and Discussion

3.1 Descriptions of crystal structures

Crystal Structure of $[Zn_2(tib)_{4/3}(L^1)_2]\cdot DMA$ (1). Single-crystal X-ray structural analysis reveals that compound **1** crystallizes in the chiral trigonal space group *P3*. The synthesis did not involve any chiral reactant, solvent or other auxiliary agent. To our surprise, the resulting crystals were not a racemic mixture, but a chiral single crystal, as evidenced by the observation of strong dichroic signal with positive cotton effect in solid-state circular dichroism (CD) (Fig. 1). It means that **1** is spontaneously resolved by crystallization. Spontaneous resolution, known as the segregation of enantiomers upon crystallization, was discovered as early as 1846 by Louis Pasteur.[16] It is still a rare phenomenon that cannot be predicted a priori because the laws of physics determining the processes are not yet fully understood.[17] The structure of **1** is comprised of two crystallographically independent 3D motifs (**α** and **β**). As shown in Fig. 2, two crystallographically independent Zn(II) centers (Zn1 in motif **α** and Zn2 in motif **β**) are both coordinated by two carboxylic O atoms from two different L^1 ligands and two N atoms from two different tib ligands to give a distorted ZnO_2N_2 tetrahedral geometry with slightly different bond lengths and bond angles (Table S1). The Zn-O/N bond lengths range from 1.926(4) Å to 2.051(4) Å, comparable with those observed in related compounds.[18]

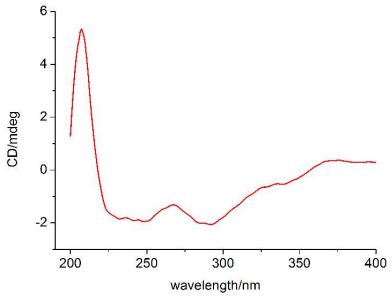

Fig. 1. Solid-state circular dichroism (CD) spectra of compound **1**

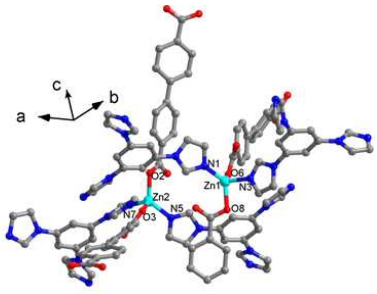

Fig. 2. A view of **1** showing the coordination environment around the Zn(II) centres. All hydrogen atoms and solvent molecules are omitted for clarity.

Chirality is often closely related with helicity in the same structure, although they are two distinct concepts.[19] The first structural feature of **1** is that the 3D framework contains helical motifs. In motif **α**, the interlaced triple-stranded homo right-handed helical chains constructed by L^1 anions and Zn1(II) atoms are circumgyrated, which is formed by the interweaving of three single-stranded chains with alternating helical parts that extend along the *c* axis with pitch length of 34.49 Å (Fig. 3a). This case is rather rare, only a few elegant 3D coordination networks consisting of triple-stranded helices hitherto have been characterized.[20] Each of two types of tib ligands coordinates to three Zn(II) atoms with a nonplanar geometry with dihedral angles of ca. 66° and 65°, respectively, resulting in the formation of 2D chiral network. Carefully, when viewed along the *a*-axis and *b*-axis, respectively, the 2D network with a honeycomb overall topology contains two types of left-handed helical chains and the pitch of each helix spans a distance of 19.11 Å (Fig. 4a). The overall 3D net is formed by the intersection, at the shared Zn1 nodes, of 1D Zn1-L^1-Zn1 helical chains and the 2D chiral $[Zn1(tib)_{2/3}]^{2+}$ layers (Fig. 5).

As determined by the TOPOS software,[21] the overall topology is characterized by a binodal (3,4)-coordinated underlying net[21] with the total point symbol of $(10^3)_2(10^6)_3$ for $(tib)_2Zn_3$ and the vertex symbols $[10_{13}\cdot10_{13}\cdot10_{13}]$ and $[10_7\cdot10_7\cdot10_8\cdot10_{10}\cdot10_{11}\cdot10_{11}]$ for two non-equivalent nodes. It belongs to the *sun2* topological type, which was detected for the first time by Sun et al.[23] Careful inspection of the network reveals that it shows self-catenation phenomenon. The catenated 10-rings are the shortest topological rings. Entanglement calculation of TOPOS shows that there are 16 types of non-equivalent circuits and they are interlocked with each other in many patterns. The most one is catenated even with 20 rings. As shown in Fig. 5, for example, each 10-ring is penetrated by two rods: one lies in two 10-rings and the other lies in three 10-rings. Thus, each 10-ring is interlocked with other five 10-rings.

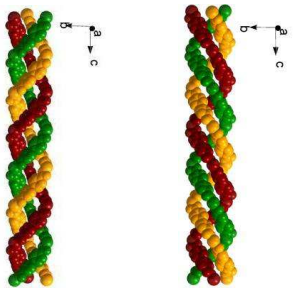

Fig.3. Space-filling view of interlaced triple-stranded (a) right-handed $[Zn1(L^1)]_n$ helical chains in motif **α**; (b) left-handed $[Zn2(L^1)]_n$ helical chains in motif **β**.

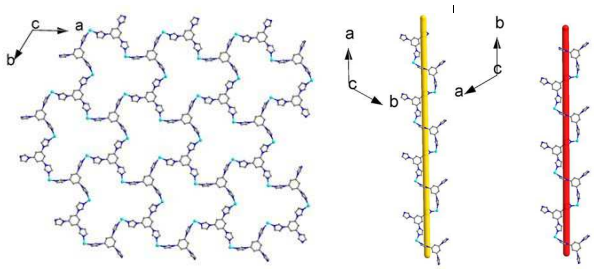

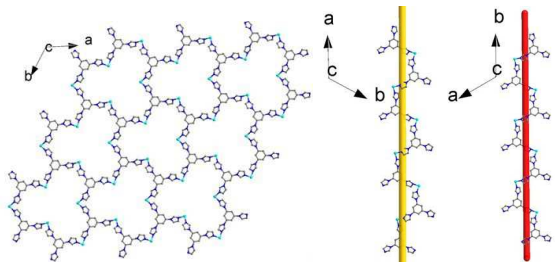

(b)

Fig. 4. Stick and spheres view of (a) 2D chiral $[Zn1(tib)_{2/3}]^{2+}$ honeycomb layer (left) containing two types of left-handed helical chains viewing along the *a*-axis (middle)and *b*-axis (right), respectively, in motif **α**; (b) 2D chiral $[Zn2(tib)_{2/3}]^{2+}$ layer (left) containing two types of right-handed helical chains viewing along the *a*-axis (middle) and *b*-axis (right), respectively, in motif **β**.

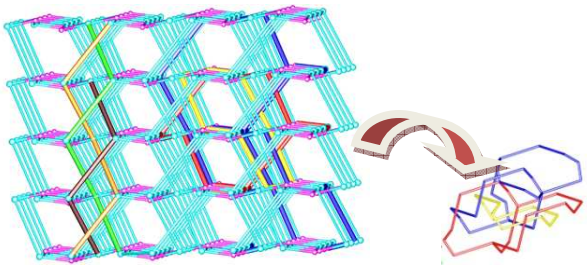

Fig. 5. Schematic description of the chiral (3,4)-coordinated self-catenated 3D motif **α**: cyan/Zn1 nodes, pink/tib ligands. One triple-stranded right-handed [Zn1(L^1)] helical chains are highlighted in green, orange and brown. One 10-ring in yellow is catenated by five other 10-rings, including three in blue and two in red.

It should be mentioned that motif **β** involving in Zn2(II) atoms also displays a 3D self-catenated binodal (3,4)-coordinated $(10^3)_2\cdot(10^6)_3$ network with helix (Fig. S1). However, the Zn2-L^1-Zn2 triple-stranded helical chains in **β** is left-handed with the same pitch rather than right-handed ones in **α** (Fig. 3b) and the 2D chiral $[Zn2(tib)_{2/3}]^{2+}$ layers contain two types of right-handed helical chains with the same pitch instead of left-handed ones in **α** (Fig. 4b). It seems that two such motifs are a pair of enantiomers. By careful inspections of two structures, we find that the difference between two kinds of L^1 anions causes that two types of helical chains are not racemic. The dihedral angle of two nonplanar benzoic rings of each L^1 anion in **α** is ca. 15.13°, however, that in **β** is ca. 15.26°. In addition, two types of tib ligands in **β** also both exhibit a nonplanar geometry, but their dihedral angles are ca. 62° and 79°, respectively, which are different from those in **α**. Accordingly, two motifs are not enantiomeric. These differences may result in the chiral of compound **1**. Remarkably, motifs **α** and **β** interpenetrate with the remaining space occupied by free DMA solvent molecules (Fig. 6). Totally, compound **1** is two-fold interpenetrating nets with Z=1+1 in that two interpenetrated nets are non-equivelent.[22] Calculations using PLATON show that compound **1** still possesses free void space estimated to be about 593.4 $Å^3$, that is 16.3% of the unit cell (after the removal of the guest molecules) in spite of interpenetration.

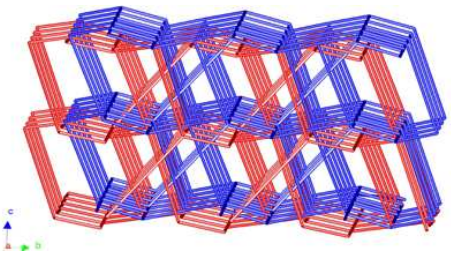

Fig. 6. Schematic view of two crystallographically independent motifs interpenetrating, red for motif **α** and blue for motif **β**. The free DMA solvent molecules are omitted for clarity.

Previously, Sun's group used $Zn(NO_3)_2\cdot6H_2O$ with the same mixed ligands to assemble one compound with the formulas of $[Zn_3(tib)_2(bpdc)_3]\cdot5H_2O$ (**A**), where bpdc = 4,4'-biphenyldicarboxylic acid = L^1, which is achiral and exhibits a 2-fold interpenetrating (3,4)-coordinated *sun2* underlying topology.[23] On the basis of the structural analysis, the compound **1** in this work is much more complicated than **A**, although they have the same topological type. The chiral and the self-catenated phenomenon in **1** may arise from the existence of two types of interlaced triple-stranded Zn-L^1-Zn helical chains and chiral 2D $[Zn(tib)_{2/3}]^{2+}$ layers, both of which are neither enantiomeric. The configurations of L^1 anions and tib ligands play key role on the ultimate network. Comparing results indicates that the solvent, temperature or reaction vessel may strongly influence the resulting structures, which also suggests that the design and prediction of coordination complexes structures are still very difficult, even if the same reactants are used. Thus, compound **1** is a chiral framework with helix characteristics having both self-catenation and interpenetration features obtained by using achiral ligands. To date, only three examples with both self-catenated and interpenetrated structural features have been characterized, which are all achiral and based on two identical nets interpenetrating. [24]

Crystal Structure of $[Zn_2(tib)_{4/3}(L^2)_2]\cdot H_2O$ (2). As compared to **1**, the H_2L^2 ligand was selected instead to react with Zn(II) ion and tib ligands, and a new compound $[Zn_2(tib)_{4/3}(L^2)_2]\cdot H_2O$ (**2**) also showing both self-catenation and interpenetration was isolated. Single-crystal X-ray structural analysis reveals that compound **2** crystallizes in trigonal space group of *R-3c*. As shown in Fig. 7, each Zn(II) ion exhibits a distorted tetrahedral environment, composed of two carboxylic O atoms from two different L^2 anions and two N atoms from two different tib ligands. The Zn-O/N bond lengths range from 1.931(5) Å to 2.007(5) Å, comparable with **1**. As shown in Fig. 8, the Zn(II) atoms are linked by L^2 anions to generate the Zn-L^2-Zn zigzag chains that span into three directions, rather than interlaced triple-stranded Zn-L^1-Zn helical chains in **1**. This may be due to the orientation of C-O-C bond. Similar to **1**, each of two types of tib ligands coordinates to three Zn(II) atoms with a nonplanar geometry with dihedral angles of ca. 74° and 78°, respectively, leading to the formation of two types of chiral 2D networks. One contains two types of left-handed helical chains and the pitch of each helix spans a distance of 18.78 Å, the other contains two types of right-handed helical chains with the same pitch, when viewed along the *a*-axis and *b*-axis, respectively (Fig. S2). Two types of chiral 2D $[Zn(tib)_{2/3}]^{2+}$ layers are arranged alternatively. The overall 3D net is formed by the intersection, at the shared Zn

nodes, of 1D Zn-L^2-Zn zigzag chains and alternative-arranged 2D $[Zn\ (tib)_{2/3}]^{2+}$ layers (Fig. 9). As determined by TOPOS software, the overall topology is a binodal (3,4)-coordinated network with the total point symbol of $(10^3)_2(10^6)_3$ for $(tib)_2Zn_3$, which is the same as **1**. However, the vertex symbols are different: they are $[10_7{\cdot}10_7{\cdot}10_7]$ and $[10_2{\cdot}10_4{\cdot}10_5{\cdot}10_5{\cdot}10_5{\cdot}10_5]$ for two non-equivalent nodes. This simplified net defines a new topology that is unobserved not only in MOFs, but also unenumerated in the electronic databases EPINET, RCSR, and TOPOS TTD.[21,25] We have deposited this topology to the TTD collection under the name *yue1*.

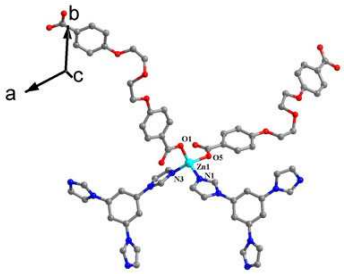

Fig. 7. A view of **2** showing the coordination environment around the Zn(II) centres. All hydrogen atoms and free water molecules are omitted for clarity.

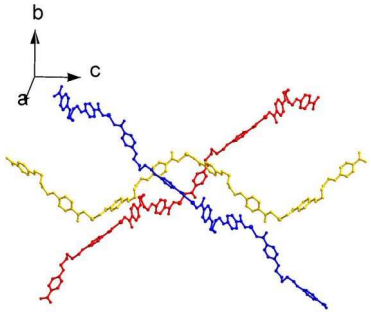

Fig. 8. A view of 1D Zn(L^2) zigzag chains that span into three directions in **2**.

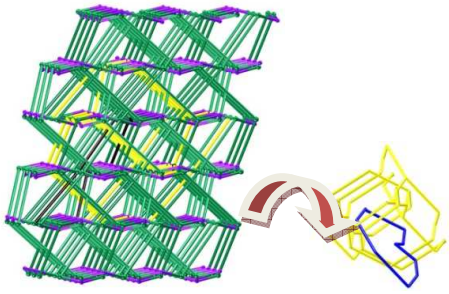

Fig. 9. Schematic description of a (3,4)-coordinated self-catenated 3D network in **2:** green/Zn nodes, purple/tib ligands. One 10-ring in blue is catenated by five other yellow 10-rings.

Self-catenation is also observed in **2**. The catenated 10-rings are the shortest in the *yue1* underlying net. Entanglement calculation of TOPOS shows that there are 4 types of non-equivalent circuits and they are interlocked with each other in many patterns. The most one is catenated even with 24 rings. As shown in Figure 8, for example, each 10-ring is penetrated by two rods: one lies in two 10-rings and the other lies in three 10-rings. Thus, each 10-ring is interlocked with other five 10-rings. Of particular interest, a pair of identical 3D single nets is interlocked with each other, thus directly leading to the formation of a 2-fold interpenetrated 3D architecture (Fig. 10). In addition, the entanglement still allows the existence of free void space occupied by the guest water. An analysis of the topology of interpenetration reveals that **2** belongs to Class IIa and Z=2; that is, two interpenetrated nets are related by a center of symmetry -1. Calculations using PLATON show that compound **2** still possesses free void space estimated to be about 2502.9 $Å^3$, that is 9.7% of the unit cell (after the removal of the guest molecules) in spite of interpenetration. Thus, compound **2** shows a new topological type and it is another example with both self-catenation and interpenetration features.

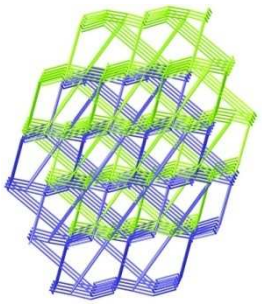

Fig. 10. Schematic view of 2-fold interpenetrated network in **2**. The free water molecules are omitted for clarity.

3.2 Metal+tib combination as a platform for new chiral and catenated structures

Analysis of the Cambridge Structural Database (release 5.35, November 2013) and the literature shows that tib ligands occur in 48 structures, out of which 22 contain Zn atoms. The coordination numbers of Zn atoms are four (most typical), five, or six; tib ligands have coordination types μ_2 or μ_3 (the latter is more preferable and realized in our complexes). Close inspection of the Zn complexes shows that the μ_2 bridge type is realized if the bridge ligands are coordinated by Zn atoms in a square-like fashion that occurs in octahedral Zn complexes. If Zn atom has coordination number four and hence its coordination figure is tetrahedral, tib ligand prefers μ_3 tripodal type.

The overall topology of Zn(four-coordinated)+μ_3-tib motif depends on other ligands L connected to Zn. If L is a prolonged ligand like 4-(2-carboxylatovinyl)benzoate,[26] L^1, or L^2, a 2D honeycomb motif emerges. If L is benzene-1,2-dicarboxylate or its substitution derivates,[23,27] different 1D, 2D, or 3D motifs can appear.

Finally, in all structures with the honeycomb Zn+tib motif and prolonged L ligands, interpenetrated networks exist. So we can conclude that the 'Zn+tib+prolonged bridge ligand' combination can give rise to a honeycomb-layer-based catenated structure with high probability. We suppose that in this combination Zn can be replaced with other *d*-metal atoms, in particular, Cd, Co, or Mn, because their honeycomb-like layers with tib ligands are known,[28] but prolonged bridge L ligands have not been used for the synthesis of such complexes so far. Moreover, as we show in this paper, length-modulated L ligands may cause chiral and achiral structures.

From the above-mentioned structural descriptions, we find Zn(II) cations, the tib ligands and the dicarboxylates show the same coordination modes or analogous configurations.

Compound **1** is a chiral structure, and **2** is an achiral framework. Therefore, we believe that the structures and properties also can be modified by changing the spacer groups, for instance, the length of the spacer. (Scheme 1).

Scheme 1

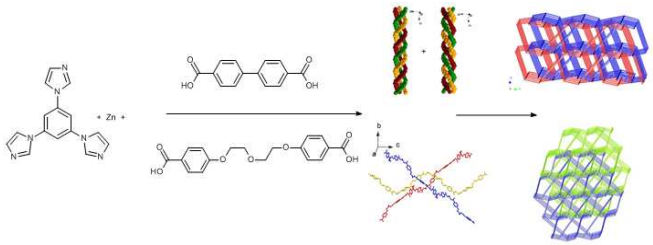

All these correlations allow us to make a conclusion that the metal+tib combination modulated by prolonged L ligands can be a good platform for new chiral and catenated structures.

3.3 Thermal Analysis

The TG analysis was performed in N_2 atmosphere on polycrystalline samples of compounds **1-2**, and the TG curves arlecules in *ca.* 85-256 ℃ (obsd 8.51%, calcd 8.17%). The solvent-free e shown in Fig. S3. Compound **1** lost lattice DMA monetwork does not decompose until *ca.*440 ℃, and then the collapse of the network of **1** occurs. Compound **2** released free water molecules in *ca.*75-155 ℃ (obsd 1.82%, calcd 1.50%), then the remaining frameworks began to decompose at *ca.*430 ℃.

3.4 Ferroelectric Properties

The space group of *P*3 of compound **1** is associated with the point group C_3, one of the ten polar point groups required for ferroelectric behavior. The dielectrical hysteresis loop along the *c* axis (the C_3 axis) direction of the randomly selected single crystal was measured. It displays ferroelectric features representing electric hysteresis loops (Fig. 11). When applied field is about 140 kV cm^{-1}, **1** shows a remnant polarization (*P*r) of ca. 0.032 μC cm^{-2} and a coercive fields (*E*c) of ca. 26.63 kV cm^{-1}. Thus, **1** does display ferroelectric behavior.

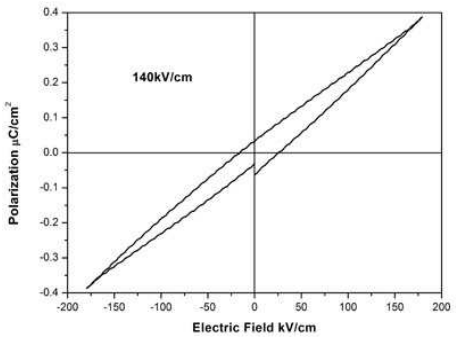

Fig. 10 Electric hysteresis loops of compound 1 under 140 Kv/cm at room temperature

3.5 Photoluminescent Properties

Photoluminescent measurements of the compounds **1-2** were carried out in the solid state at room temperature (Fig. S4). It can be seen that the intense broad photoluminescence emission at 411 nm (λ_{ex}=360 nm) for **1** and 463 nm (λ_{ex}=370 nm) for **2** are exhibited, which may exist as a mixture characteristics of intraligand and ligand-to-ligand charge transitions, since Zn(II) is difficult to oxidize or to reduce due to its d^{10} configuration.[29]

4. Conclusions

In conclusion, two new Zn(II) coordination complexes are obtained by using 1,3,5-tris(1-imidazolyl)benzene and different dicarboxylic acids. Compounds **1** and **2** both have interpenetration and self-catenation characters. Compound **1** is chiral, which is composed of two crystallographically independent 3D motifs, each containing interlaced triple-stranded right- and left-handed Zn–L^1–Zn helical chains and 2D chiral $[Zn(tib)_{2/3}]^{2+}$ layers, respectively, and showing binodal (3,4)-coordinated $(10^3)_2{\cdot}(10^6)_3$ topology. Compound **2** exhibits a new binodal (3,4)-coordinated $(10^3)_2{\cdot}(10^6)_3$ topology, with the vertex symbols different from those in **1**. As expect, compounds **1-2** have photoluminescence behaviors and compound **1** has ferroelectric behavior. The results presented here inspired us that the rigid ligands can be used to build homochiral MOFs with homo-handed helical chains, and further proved that long ligand is a good choice for the construction of entangled structures.

Acknowledgment

This work was supported by the Science and technology basic research item of Qingdao City (12-1-4-2-(24)-jch). V.A.B. thanks Russian government (grant No. 14.B25.31.0005) and Russian Foundation for Basic Research (grant No. 13-07-00001) for support.

Notes and references

[a] *College of Chemical Science and Engineering, Qingdao University, 308 Ningxia Road, Qingdao 266071, China. Tel: +86-532-85955529; E-mail: wangyue@qdu.edu.cn.*
[b] *Samara Center for Theoretical Materials Science (SCTMS), Samara State University, Ac. Pavlov St. 1, Samara 443011, Russia. E-mail: blatov@samsu.ru*
[c] *Chemistry Department, Faculty of Science, King Abdulaziz University P. O. Box 80203, Jeddah 21589, Saudi Arabia.*
[d] *Chemistry Department, Nankai University, 300071, Tianjin, China*

† Electronic Supplementary Information (ESI) available: [CCDC 1001743-1001744 for ESI and crystallographic data in CIF format, general characterization (TG, ferroelectric and photoluminescence) and additional structural figures and tables]. See DOI: 10.1039/b000000x/

1 (a) O. M. Yaghi, M. O'Keeffe, N. W. Ockwig, H. K. Chae, M. Eddaoudi, J. Kim, *Nature*, 2003, **423**, 705; (b) S. Kitagawa, R. Kitaura, S. Noro, *Angew. Chem., Int. Ed.*, 2004, **43**, 2334.

(2) (a) L. Q. Ma, C. Abney, W. B. Lin, *Chem. Soc. Rev*. 2009, **38**, 1248; (b) W. W. Zhou, J. T. Chen, G. Xu, M. S. Wang, J. P. Zou, X. F. Long, G. J. Wang, G. C. Guo, J. S. Huang, *Chem. Commun*. 2008, 2762; (c) Z. G. Guo, R. Cao, X. Wang, H. F. Li, W. B. Yuan, G. J. Wang, H. H.Wu, J. Li, *J. Am. Chem. Soc*. 2009, **131**, 6894; (d) T. Hang, W. Zhang, H.Y. Ye, R. G. Xiong, *Chem. Soc. Rev*, 2011, **40**, 3577; (e) W. Kaneko, S. Kitagawa, M. Ohba, *J. Am. Chem. Soc*. 2007, **129**, 248.

(3) (a) L. Carlucci, G. Ciani, P. Macchi, D. M. Proserpio, *Chem. Commun.*, 1998, 1837; (b) L. Carlucci, G. Ciani, D. M. Proserpio, S. Rizzato, *Chem. Commun.*, 2000, 1319; (c) C. J. Kepert, M. J. Rosseinsky, *Chem. Commun.*, 1998, 31; (d) R. G. Xiong, J. L. Zuo, X. Z. You, B. F. Abrahams, Z. P. Bai, C. M. Che, H. K. Fun, *Chem. Commun.*, 2000, 2061; (e) A. J. Blake, N. R. Champness, P. A. Cooke, J. E. B. Nicolson, *Chem. Commun*., 2000, 665.

(4) (a) M. Kondo, M. Miyazawa, Y. Irie, R. Shinagawa, T. Horiba, A. Nakamura, T. Naito, K. Maeda, S. Utsuno, F. Uchida, *Chem. Commun*., 2002, 2156; (b) E. Gao, Y. Yue, S. Bai, Z. He, C. Yan, *J. Am. Chem. Soc*., 2004, **126,** 1419; (c) Y. Q. Lan, S. L. Li, X. L.

Wang, K. Z. Shao, D. Y. Du, Z. M. Su, E. B. Wang, *Chem. Eur. J.* 2008, **14**, 9999.
(5) (a) Y. Ma, Z. B. Han, Y. K. He, L. G. Yang, *Chem. Commun*., 2007, 4107; (b) Q. X. Yao, W. M. Xuan, H. Zhang, C. Y. Tu, J. Zhang, *Chem. Commun*., 2009, 59; (c) Z. Su, M. S. Chen, J. Fan, M. Chen, S. S. Chen, L. Luo, W. Y. Sun, *CrystEngComm*, 2010, **12**, 2040.
(6) (a) C. Janiak, *Angew. Chem., Int. Ed*. 1997, **36**, 1431; (b) M. Eddaoudi, H. Li, O. M. Yaghi, *J. Am. Chem. Soc.* 2000, **122**, 1391; (c) M. J. Zaworotko, *Angew. Chem., Int. Ed*. 2000, **39**, 2113; (d) S. Noro, S. Kitagawa, M. Kondo, K. Seki, *Angew. Chem., Int. Ed*. 2000, **39**, 2081.
(7) (a) S. R. Batten, R. Robson, *Angew. Chem., Int. Ed*. 1998, **37**, 1460; (b) S. R. Batten, *CrystEngComm* 2001, **3**, 67; (c) L. Carlucci, G. Ciani, D. M. Proserpio, *Coord. Chem. Rev*. 2003, **246**, 247; (d) V. A. Blatov, L. Carlucci, G. Ciani, D. M. Proserpio, *CrystEngComm* 2004**,** **6**, 377; (e) I. A. Baburin, V. A. Blatov, L. Carlucci, G. Ciani, D. M. Proserpio, *J. Solid State Chem*. 2005, **178**, 2452; (f) I. A. Baburin, V. A. Blatov, L. Carlucci, G. Ciani, D. M. Proserpio, *Cryst. Growth Des*. 2008, **8**, 519.
(8) (a) B. F. Abrahams, S. R. Batten, M. J. Grannas, H. Hamit, B. F. Hoskins, R. Robson, *Angew. Chem., Int. Ed.*, 1999, **38**, 1475; (b) M. L. Tong, X. M. Chen, S. R. Batten, *J. Am. Chem. Soc.*, 2003, **125**, 16170; (c) M. R. Montney, S. M. Krishnan, N. M. Patel, R. M. Supkowski, R. L. LaDuca, *Cryst. Growth Des.*, 2007, **7**, 1145; (d) D. P. Martin, R. L. LaDuca, *Inorg. Chem*., 2008, **47**, 9754.
(9) (a) P. Jensen, D. J. Price, S. R. Batten, B. Moubaraki, K. S. Murray, *Chem. Eur. J*., 2000, **6**, 3186; (b) X. Li, R. Cao, D. F. Sun, W. H. Bi, D. Q. Yuan, *Eur. J. Inorg. Chem.*, 2004**,** 2228; (c) X. L. Wang, C. Qin, E. B. Wang, Z. M. Su, L. Xu, S. R. Batten, *Chem. Eur. J.*, 2006, **12**, 2680; (d) J. Yang, J. F. Ma, Y. Y. Liu, S. R. Batten, *CrystEngComm* 2009, **11**, 151.
(10) (a) Y. Qi, F. Luo, Y. X. Che, J. M. Zheng, *Cryst. Growth Des.* 2008, **8**, 606; (b) Y. Qi, Y. X. Che, J. M. Zheng, *Cryst. Growth Des*. 2008, **8**, 3602; (c) K. M. Blake, J. S. Lucas, R. L. LaDuca, *Cryst. Growth Des*. 2011, **11**, 1287; (d) Q. X. Jia, Y. Q. Wang, Q. Yue, Q. L. Wang, E. Q. Gao, *Chem. Commun*., 2008, 4894; (e) X. J. Ke, D. D. Li, M. Du, *Inorg. Chem. Commun*. 2011, **14**, 788.
(11) X. H. Bu, M. L. Tong, H. C. Chang, S. Kitagawa, S. R. Batten, *Angew. Chem., Int. Ed*. 2004, **43**, 192.
(12) B. Gmez-Lor, E. Gutirrez-Puebla, M. Lglesias, M. A. Monge, C. Ruiz-Valero, N. Snejko, *Chem. Mater.* 2005, **17**, 2568.
(13) Y. Qi, F. Luo, S. R. Batten, Y. X. Che, J. M. Zheng, *Cryst. Growth Des.* 2008, **8**, 2806.
(14) (a) Z. Su, Y. Song, Z. S. Bai, J. Fan, G. X. Liu, W. Y. Sun, *CrystEngComm*, 2010, **12**, 4339; (b) J. Fan, M. H. Shu, T.-aki Okamura, Y. Z. Li, W. Y. Sun, W. X. Tang, *New J. Chem.*, 2003, **27**, 1307.
(15) (a) B. Q. Ma, K. L. Mulfort, J. T. Hupp, *Inorg. Chem*., 2005**,** **44**, 4912; (b) J. Fan, W. Y. Sun, T.-aki Okamura, W. X. Tang, N. Ueyama, *Inorg. Chem.*, 2003, **42**, 3168.
(16) L. Pasteur, Ann. Chim. Phys. 1848, 24, 442.
(17) (a) S. L. Li, Y. Q. Lan, J. S. Qin, J. F. Ma, J. Liu, J. Yang, *Cryst. Growth Des.* 2009, **9**, 4142; (b) C. Y. Chen, P. Y. Cheng, H. H. Wu, H. M. Lee, *Inorg. Chem*. 2007, **46**, 5691; (c) E. Q. Gao, Y. F. Yue, S. Q. Bai, Z. He, C. H. Yan, *J. Am. Chem. Soc.* 2004, **126**, 1419.
(18) Y. Qi, Che, Y. X. J. M. Zheng, *CrystEngComm*, 2008, **10**, 1137.
(19) (a) J. Zhang, X. H. Bu, *Chem. Commun*., 2009, 206; (b) L. Q. Ma, W. B. Lin, *J. Am. Chem. Soc.*, 2008, **130**, 13834; (c) J. S. Heo, Y. M. Jeon, C. A. Mirkin, *J. Am. Chem. Soc.*, 2007, **129**, 7712; (d) S. F. Mason, Molecular Optical Activity and the Chiral Discriminations, Cambridge University Press, Cambridge, 1982.
(20) (a) D. R. Xiao, E. B. Wang, H.Y. An, Y. G. Li, Z. M. Su, C. Y. Sun, *Chem. Eur. J.* 2006, **12**, 6528; (b) S. Q. Zang, Y. Su, Y. Z. Li, Z. P. Ni, H. Z. Zhu, Q. J. Meng, *Inorg. Chem*. 2006, **45**, 3855; (c) X. H. Huang, T. L. Sheng, S. C. Xiang, R. B. Fu, S. M. Hu, Y. M. Li, X. T. Wu, *Inorg. Chem*. 2007, **46,** 497; (d) Y. Q. Xu, J. S. Xi, W. Wei, Y. N. Chi, C. W. Hu, *Inorg. Chem. Commun*. 2010, **13**, 852.
(21) E. V. Alexandrov, V. A. Blatov, A. V. Kochetkov, D. M. Proserpio, *CrystEngComm* 2011, **13**, 3947; V. A. Blatov, *Struct. Chem*., 2012, **23**, 955; http://www.topos.samsu.ru.
(22) V. A. Blatov, L. Carlucci, G. Ciani, D. M. Proserpio, CrystEngComm 2004, **6**, 377.
(23) D. Sun, Z. H. Yan, V. A. Blatov, L. Wang, D. F. Sun, *Cryst. Growth Des.* 2013, **13**, 1277.
(24) (a) T. Schareina, C. Schick, B. F. Abrahams, R. Kempe, *Z. Anorg. Allg. Chem.*, 2001, **627**, 1711; (b) Z. H. Zhang,; S. C. Chen, J. L. Mi, M. Y. He, Q. Chen, M. Du, *ChemComm* 2010, **46**, 8427; (c) X. L. Wang, Y. Q. Chen, Q. Gao, H. Y. Lin, G. C. Liu, J. X. Zhang, A. X. Tian, *Cryst. Growth Des*., 2010, **10**, 2174.
(25) (a) M. O'Keeffe, M. A. Peskov, S. J. Ramsden, O. M. Yaghi, *Acc. Chem. Res.* 2008, **41**, 1782 database available at http://rcsr.anu.edu.au/. (b) S. J. Ramsden, V. Robins, S. T. Hyde, *Acta Crystallogr.* 2009, **A65**, 81 database available at http://epinet.anu.edu.au.
(27) Z. Su, J. Fan, W. Y. Sun, *Inorg. Chem. Commun*. 2013, **27**, 18.
(28) (a) Z. Su, J. Xu, J. Fan, D. J. Liu, Q. Chu, M. S. Chen, S. S. Chen, G. X. Liu, X. F. Wang, W. Y. Sun, *Cryst. Growth Des*. 2009, **9**, 2801; (b) Z. Su, J. Fan, T. Okamura, W. Y. Sun, *Chin. J. Chem*. 2012, **30**, 2016.
(29) (a) L. Wang, Z. H. Yan, Z. Xiao, D. Guo, W. Wang, Y. Yang, CrystEngComm 2013, **15**, 5552.
(26) S. Zhi, J. Fan, T-aki Okamura, M. S. Chen, S. S. Chen, W. Y. Sun, N. Ueyama, *Cryst. Growth & Des*., 2010, **10**, 1911.